Amitriptyline Accelerates SERT Binding Recovery Rate in MDMA-Induced Rat Model: *In Vivo* 4-[^{18}F]-ADAM PET Imaging

Skye Hsin-Hsien Yeh (skyeyeh@live.com)
National Yang-Ming University https://orcid.org/0000-0002-7495-1146
Chuang-Hsin Chiu
Tri-Service General Hospital
Yu-Yeh Kuo
Hsin Sheng College of Medical Care and Management
Chi-Jung Tsai
Taipei Medical University Hospital
Tsung-Hsun Yu
National Yang Ming Chiao Tung University
Wen-Sheng Huang
Taipei Medical University Hospital
Kuo-Hsing Ma
National Defence College: National Defence University

Research Article

Keywords: 4-[18F]-ADAM, MDMA, SERT, amitriptyline

Posted Date: October 7th, 2021

DOI: https://doi.org/10.21203/rs.3.rs-933822/v1

Abstract

Background Numerous studies have confirmed that 3, 4-Methylenedioxymethamphetamine (MDMA) produces long-lasting changes to the serotonergic system and decreases the density of the serotonin reuptake transporter (SERT). However, amitriptyline (AMI) is a potent neuroprotector that can cause devastating neuropathologic injury. Use of 4-[^{18}F]-ADAM, a SERT-specific radionuclide as a molecular imaging agent, facilitates longitudinal, non-invasive assessment of SERT activity/expression post-MDMA. We used 4-[^{18}F]-ADAM PET imaging to access the longitudinal alteration of SERT binding and evaluate the synergistic neuroprotective effect of MDMA and SERT inhibition by AMI in rat model.

Materials and Methods The adult male Sprague–Dawley (SD) rats are grouped into four according to drug administration (Group 1: saline, Group 2: MDMA 10mg/kg *i.p.*, Group 3: MDMA 10mg/kg *i.p.* with AMI 5 mg/kg *i.p.*, Group 4: AMI 5 mg/kg *i.p.*). All drugs were administrated twice daily for 4 successive days (Day 1 to Day 4). Post-drug 4-[^{18}F]-ADAM PET scans were performed on day 14, day 21 and day 28 to measure the SERT occupancy/recovery. After the last PET imaging, SERT-positive cells were measured quantitatively using immunochemical staining.

Results In response to MDMA treatment regimens, SERT binding was significantly reduced in rat brain. Recovery rate (normalized to baseline) in the MDMA group, at day 14 was 64.34% ± 2.05%, progressively increased to 70.70% ± 3.96% at day 28. Recovery rate in the MDMA group varies based on region-specific. AMI dramatically increased SERT binding in all brain regions, enhancing average ~24% recovery rate at day 14 when compared with the MDMA group (MDMA 64.34% ± 2.05% vs. MDMA+ AMI 87.76% ± 2.98%), reaching 84.38% ± 2.05% at day 28. The immunochemical staining revealed that MDMA treatment reduced SERT immunoactivity densities in all brain regions, whereas AMI markedly increased the serotonergic fiber density after MDMA-induction that confirmed the PET findings.

Conclusions Using *in vivo* longitudinal PET imaging, we demonstrated that SERT recovery was positively correlated with the duration of MDMA abstinence, implying the lower SERT densities in MDMA-induced rats reflected neurotoxic effects, varied region-specific, and reversible. AMI globally accelerated the recovery rate of SERT binding and increased SERT fiber density with possible neuroprotective effects.

Background

3, 4-Methylenedioxymethamphetamine (MDMA) is a ring-substituted that has a chemical structure similar to amphetamine. MDMA comprises of mescaline that has amphetamine stimulant having hallucinogenic effects [1]. Amphetamine is phenylethylamine derivatives. Its chemical properties comprise monoamine neurotransmitters and natural hallucinogenic compounds, such as mescaline and cathinone. Thus, the amphetamine produces the central nervous system stimulant and hallucinogenic effects [2].

MDMA affects peripheral and monoamine that plays an important neurotrophic role in the maturation of the central nervous system. Some studies conducted MDMA in vivo stimulation in brain tissue of rats, using serotonin outflow and dopamine to compare their multiple effects [3]. Some studies have pointed

out that the interaction between MDMA and monoamine transporter facilitates the end of the cell synaptic neurons release serotonin, dopamine, and norepinephrine [2, 4]. Thus, MDMA-induced monoamine transporter on neurons is the pharmacology and toxicity of biological targets. From the perspective of the MDMA-induced neurotoxicity, some studies argue that when MDMA is combined with the high-affinity monoamine transporter, its MDMA affinity for the serotonin transporter is much higher than other monoamine class transporters [5]. When the MDMA and serotonin transporter bind after a certain position, they transport to the presynaptic serotonin neurons. Thereby, the serotonin transporter massively releases serotonin into the synaptic cleft [6]. Presently, no clear conclusion reveals how MDMA causes a massive release of serotonin mechanisms. However, it is confirmed that MDMA can cause a massive release of serotonin in the brain after its rapid decline and produce depletion of the forebrain in rodents and primates, and this phenomenon in rodents and primates can be observed [7, 8, 9].

Many studies have confirmed that MDMA can cause selective damage to rodents and primate's serotonin systems. In addition, MDMA has been demonstrated to reduce serotonin levels, serotonin reuptake transporter (SERT), and the amount of serotonin synthesis tryptophan hydroxylase important to enzymes in the use of MDMA after have significantly reduced [10, 11, 12, 13]. These phenomena occur because of MDMA effect on serotonin neurons injury and MDMA inhibition of the presynaptic neuron into the tryptophan hydroxylase enzyme and the disintegration of monoamine oxidase-B (MAO-B). Serotonin concentrations rise sharply after MDMA administration but quickly dropped in a few moments [14, 15].

Nuclear medicine is a vital imaging technique to detect molecular serotonin transporter distribution in the central nervous system. In addition, serotonin is important in the regulation mechanism, providing important information about the diagnosis and treatment. *In vivo* nuclear medicine imaging of the serotonin transporter uses the quantitative technique as a research method. Positron emission tomography technology, a kind of serotonin transporter in contrast to agents [^{11}C]DASB, can have long-term use of MDMA in the human brain serotonin system. The results showed a significant reduction in all brain regions of serotonin transporter [16, 17]. By administering 5mg/kg MDMA subcutaneously twice daily for four consecutive days, the MDMA-induced decrease in brain SERT levels, which could persist for over four years in primates [13].

As discussed above, SERT is one of the pharmacology and toxicity of MDMA biological targets. The SERT involvement in the MDMA-induced neurotoxicity mechanism has been extensively studied [18, 19, 20]. The neuroprotective effect of selective serotonin reuptake inhibitors (SSRIs) (i.e., fluoxetine) has been studied in a rat model after MDMA intoxication [3, 21]. In addition, co-administration of MDMA with SSRIs (e.g., fluoxetine and citalopram) can prevent subsequent extracellular oxidative stress [22], long-term serotonin depletion and serotonin uptake site decrease, indicating that free radical production might occur following SERT activation by MDMA [23, 24, 25].

Amitriptyline (AMI) is one of the earliest members of the tricyclic antidepressants family. AMI functions as SERT inhibitor (ki = 1 nM), norepinephrine transport reuptake (NET) inhibitors (ki = 35 nM), and dopamine transport reuptake (DAT) inhibitor (ki = 3780 nM) [26, 27]. AMI is also effective for the

therapeutic of some mental disorders and treatment of neuropathic pain [28, 29] AMI seems to be highly more effective than newer SSRIs [30, 31]. Regarding anti-depressant actions, AMI induces dose-dependent pluripotent actions of this drug [27, 32]. Interestingly, several studies confirm that AMI elicits strong neurotrophic activity via a productive interaction with the brain-derived neurotrophic factor and neurotrophin tyrosine kinase receptor B (TrkB) system [28, 29, 33, 34]. Kamińska et al., (2018) reported that chronic treatment with AMI in a unilaterally 6-hydroxydopamine lesion rat model increased dopamine levels. However, it decreased SERT and NET levels in the striatum and substantia nigra as well as improving motor dysfunction [35]. However, the *in vivo* interaction between SERT and AMI or the neuroprotection of AMI in MDMA-induced serotonin neurotoxicity remains unknown.

In this study, we developed a selective positron emission tomography (PET) imaging agent for the serotonin transporter, 4-[^{18}F]-ADAM, demonstrating its selectivity, specificity, and safety using rodent or primate models [36–40] and human study [41]. Furthermore, we demonstrated that fluoxetine produced long-lasting protection against MDMA-induced neurotoxicity [20].

In light of these finds, this study aims to use PET 4-[^{18}F]-ADAM to assess (1) the *in vivo* interaction between SERT and AMI, (2) the long-term neuronal damage or recovery of SERT after MDMA administration, and (3) the evaluation of AMI against MDMA neurotoxicity in rat brain.

Materials And Methods

Animals

Adult male Sprague–Dawley (SD) rats (250–300 g in weight) were housed at the National Defense Medical Center (Taipei, Taiwan) in animal facilities and maintained under light/dark cycle (from 7:00 AM to 7:00 PM) with a constant temperature of 23 ± 2°C. All experimental procedures were performed in compliance with the Institutional Animal Care and Use Committee guidelines at the National Defense Medical Center, Taipei, Taiwan, R.O.C. (IAUIC number 10–093).

Drug treatments and study design

MDMA (purity, 98%) was obtained from the Investigation Bureau of Taiwan, and AMI was purchased from Sigma-Aldrich (St. Louis, MO). MDMA and AMI were dissolved in saline (0.9% NaCl) at a final concentration of 10 and 5 mg/ml, respectively. Rats were treated with saline or AMI [5 mg/kg, subcutaneously (s.c.)], followed by saline or MDMA (twice a day for 4 consecutive days, 10 mg/kg, s.c.).

Rats were grouped as normal control (a saline injection, $n = 6$ for each time point), MDMA (saline followed by MDMA injection, $n = 6$ for each time point), AMI with MDMA (AMI followed by MDMA injection, $n = 6$ for each time point), AMI (AMI followed by saline injection, $n = 6$ for each time point).

The experiment was conducted using 4-[^{18}F]-ADAM PET imaging to measure SERT occupancy by amitriptyline and MDMA, as a method to gauge *in vivo* SERT binding of AMI and MDMA. The

experimental design is schematically shown in Fig. 1. Baseline 4-[^{18}F]-ADAM PET scans were conducted when the animals were free of any drug treatment. A week after the baseline scans, 24 rats were randomly assigned to 4 treatment groups injected intravenously (i.v.) with either vehicle (saline, *i.p.*) or MDMA (10 mg/kg, *s.c.*) or MDMA (10 mg/kg) with AMI (5 mg/kg, *s.c.*) subcutaneously (*s.c.*). All drugs were administrated twice a day for 4 successive days (Day 1 to Day 4). Post-drug 4-[^{18}F]-ADAM PET scans were performed on day 14, day 21 and day 28 to measure the SERT occupancy/recovery.

Radiopharmaceutical

The 4-[^{18}F]-ADAM was synthesized in an automated synthesizer as described previously. Briefly, nucleophilic fluorination of N,N-dimethyl-2-(2,4-dinitroph -enylthio) benzylamine in dimethyl sulfoxide with dried potassium [^{18}F]fluoride/ Kryptofix 2.2.2 at 120°C is reduced with Cu (OAc)2-NaBH4 in EtOH at 78°C. Purification with high-performance liquid chromatography (HPLC) produced the desired compound with a radiochemical yield (EOS) of ~ 3%, in a synthesis period of 120 min. The radiochemical yield of 4-[^{18}F]-ADAM increased to ~ 15% when using a different precursor and synthesized manually [37]. The chemical and radiochemical purities were > 95%, and the specific activity was > 3 Ci/μmol (111 GBq/μmol).

Image data acquisition and analyses

Imaging was performed according to a previous report [36] with minor modifications. Rats were anesthetized by passive inhalation of isoflurane/oxygen mixture (5% isoflurane for induction and 1% for maintenance). After 60 minutes of administration of 4-[^{18}F]-ADAM (14.8–18.5 MBq; 0.4–0.5 mCi) via tail vein, the static PET images were acquired for 30 min using a Concorde R4 Microsystem (Knoxville, TN, USA), which produced 63 image slices over a 7.89-cm axial field of view, with a slice thickness of approximately 1.25 mm. All images were reconstructed with the Ordered Subset Expectation Maximum (OSEM) algorithm, producing a 128 × 128-pixel image matrix, 16 subsets, four iterations, and a Gaussian filter. Then, images were reconstructed by the Fourier rebinning algorithm and two-dimensional filtered back-projection, applying a ramp filter cutoff using the Nyquist frequency. The reconstructed images were analyzed with PMOD (PMOD Technologies, Switzerland) to measure standardized uptake value (SUV) in various brain regions. Volumes of interest of the striatum, auditory cortex, cingulate cortex, visual cortex, hippocampus anterodorsal, hippocampus posterior, hypothalamus, thalamus, and Cerebellum were drawn manually on the reconstructed PET images, using a MRI-based rat brain atlas with PMOD (PMOD Technologies, Switzerland). The regional radioactivity concentrations (KBq/mL) of 4-[^{18}F]-ADAM PET were estimated from the maximum pixel values within each ROI and expressed as SUV.

The final data were expressed as specific uptake ratios (SURs), expressed as ($SUV_{target\ region}$ - $SUV_{cerebellum}$)/ $SUV_{cerebellum}$. The SERT recovery rate was calculated as ($SUVR_{post-drug}$ -$SUV_{baseline}$) x 100%.

Immunohistochemistry

At the latest time of PET imaging, rats (n = 3 pre group) were anesthetized with 4% chloral hydrate [1 ml/kg, intraperitoneally (i. p.)], and perfused through the ascending aorta with 0.9% normal saline,

followed by 4% paraformaldehyde in 0.1Mphosphate-buffered saline (PBS), pH 7.4.

Brains were removed, postfixed in the same fixative for 2 h, and cryoprotected overnight in a solution of 30% sucrose in 0.1 M PBS at 4°C. Sagittal sections (30 μm) cut by cryostat (Leica CM 3050, Leica Microsystems Nussloch, GmbH, Nussloch, Germany) were rinsed in PBS, incubated in 1% H_2O_2 in PBS for 30 min, washed extensively, incubated in blocking solution (1% normal goat serum in PBS 0.1 M plus 1% Triton X-100) to reduce background. Sagittal sections (30 μm) were also incubated over three nights at 4°C with rabbit anti-SERT antibody (1:2000; Chemicon International, Temecula, CA), rinsed, and incubated with goat anti-rabbit biotinylated IgG (1:200; Vector, Burlingame, CA) for 1 h. Afterward, sagittal sections were incubated with avidin-biotin complex (1:200; Vectastain ABC kit, Vector) for 0.5 h, washed, exposed to 0.05% diaminobenzidine (dissolved in 0.1% H_2O_2 in 0.05 M Tris buffer, pH 7.6) for 10 min, washed three times with distilled water, and mounted on gelatin-coated glass slides.

A semiquantitative assessment of the protein of interest expression was carried out based on the number of cells that showed nuclear expression of each SERT marker over 5 non-overlapping microscopic fields (at ×100 microscope objective magnification) according to:

0 = absent, less than 5% immunopositive neurons seen,

1 = rare, 10–20% immunopositive neurons per field,

2 = mild, 20–40% mildly or moderately positive neurons per field,

3 = moderate, 40–60% moderately or strongly positive neurons per field,

4 = strong, more than 80% strongly positive neurons per field.

A percentage score for each case was calculated as:

Actual rating x 100/maximal score (i.e., a rating value of 4).

$$\text{Percentage of positive signal} = \frac{\text{Sum of score of the group}}{\text{Number of case} \times \text{maximal score } 4} \times 100\%$$

raphe nuclei

Statistical analysis

Specific uptake rate differences of the two groups were compared using T-test or one-way analysis of variance (One-way ANOVA), posthoc Bonferroni adjustment. *P*-value less than 0.05 (*, #), or less than 0.01 (**, # #) or less than 0.005 (***, # # #) indicates significant difference. Data expressed as mean ± standard deviation (mean ± SD).

Result

SERT recovery shows region-specific and time-dependent

Figure 2A is the illustration of the location of the brain regions was used to estimate the SERT binding of 4-[^{18}F]-ADAM. The 3D 4-[^{18}F]-ADAM PET images in the rat brain are shown in Fig. 2B-C. Brain uptake of 4-[^{18}F]-ADAM in all regions was significantly lower in rats pretreated with MDMA than in control rats from day 14 to day 28 (second row). However, the uptake in the control groups was similar in each imaging data (top row). In the baseline, the hypothalamus showed the highest 4-[^{18}F]-ADAM uptake followed by the thalamus, striatum, hippocampus posterior, motor cortex, cingulate cortex, hippocampus anterodorsal, auditory cortex, and visual cortex (Fig. 3 **black line**). In all brain regions, the SURs in the MDMA group significantly decreased up to day 28 (Fig. 3 **red line**). Detailed results were summarized in Table 1.

After normalized to the baseline value, we calculated the SERT recovery rate in each time point. Figure 4 showed that the recovery rate at the control group remained relatively flat (**black line**); whereas the MDMA group appeared at its lowest recovery rate at day 14 (64.34% ± 2.05%) and slightly increased at day 21 (71.11% ± 1.96%) to day 28 (70.70% ± 3.96%) (**red line**). According to the SERT recovery rate, from day 14 to day 28, brain regions of the MDMA group averagely divided into three classifications: Low recovery rate (< 50%)- thalamus, Mid recovery rate (< 65%)- hypothalamus, hippocampus anterodorsal and Hippocampus Antero Dorsal, and High recovery rate (< 80%)- cingulate cortex, motor cortex, auditory cortex, striatum, and visual cortex. Detailed results were summarized in Table 2.

Amitriptyline Accelerated SERT Level recovery after MDMA induction

In all brain regions, co-administration of AMI with MDMA resulted in higher 4-[^{18}F]-ADAM uptake compared to the MDMA group (Fig. 2B-C). At day 14, the SURs of 7 of 9 regions showed significant difference in the two groups ($p < 0.05 \sim p < 0.005$). AMI dramatically increased 4-[^{18}F]-ADAM uptake in all brain regions (Fig. 3 blue line), which enhanced the average ~ 24% recovery rate at day 14 when compared with the MDMA group (MDMA 64.34% ± 2.05% *vs.* MDMA + AMI 87.76% ± 2.98%) (Fig. 4 blue line). Thus, the effect of MDMA induction or self-recovery rate varied in different regions. It seemed that AMI globally accelerated the SERT recovery rate from day 14 and then reached 84.38% ± 2.05% at day 28. Detailed results were summarized in Tables 1 and 2.

Amitriptyline did not affect normal brain

Since AMI was a non-selective SERT inhibitor, we further tested whether it altered normal brain SERT levels. The results showed that pre-treatment with AMI alone slightly decreased 4-[^{18}F]-ADAM uptake in all brain regions. However, no significant effect is noted regarding the curves of SURs or recovery rate of the AMI group, showing a similar pattern with the controls (Fig. 2B-C, Fig. 3–4 **green line**). Detailed results were summarized in Tables 1 and 2.

AMI markedly increased the serotonergic fiber density after MDMA-induction

The results of SERT immunohistochemical localization were obtained to compare *in vivo* PET images. A dense meshwork of fibers and high densities of SERT labeling was found in all brain regions in the control group (Fig. 5 **left panel**). Widespread heterogeneous distribution of SERT immunoreactivity was observed in the striatum, frontal cortex, and dorsal raphe (midbrain). A high dense of SERT-expressing fibers were found in the hypothalamus and thalamus in control animals (Fig. 5 **left panel**). In contrast to the control group, MDMA treatment reduced densities of SERT immunoactivity in all brain regions (Fig. 5 **second panel**). However, co-administration of MDMA with AMI restored the SERT-expressing immunoactivity (Fig. 5 **middle panel**). Similar to PET results, all brain regions of the AMI group showed a slight reduction of SERT immunoreactivity when compared with the controls. However, no significant difference is observed (Fig. 5 **right panel**).

From the outcome of the quantitative analysis, there is a decrease of 37–61% in SERT immunoreactivity of the striatum, frontal cortex, midbrain, hypothalamus, and thalamus within MDMA-induced brain relative to those of the control rats (***$p < 0.005$) (Fig. 6). Co-administration with AMI significantly increased SERT immunoactivity (##$p < 0.01$- ###$p < 0.005$) (Fig. 6). Treatment with AMI alone did not affect the SERT-expressing signal (Fig. 6).

Discussions

Using a selective SERT PET radiotracer, we monitored a long-term SERT occupancy/recovery *in vivo* and evaluated the AMI neuroprotection after MDMA induction. Our results showed that acute and repeated administration of MDMA significantly induced SERT reduction levels in all regions at day 14 compared to the controls, which were supported by previous studies, revealing that the effect of MDMA on SERT binding was a robust finding in rodents [13, 20, 42, 43, 44]. Those reports indicate that the effect of MDMA on SERT binding is a robust finding in rodent.

Regarding the long-term effects of MDMA exposure, we further investigated the effect of the duration of ecstasy abstinence on the SERT binding by examining the reversibility of the *in vivo* SERT binding during the period of abstinence from MDMA administration. We found that neurotoxicity induced by MDMA in rat brain was regional-specific, reflecting the varied SURs or progression of the self-recovery rate of SERT. In the study period (28 days), we found the regions, such as the thalamus, hypothalamus, hippocampus anterodorsal, and hippocampus anterodorsal (low or mid-self-recovery rate), had relatively slower self-recovery progression compared to cingulate cortex, motor cortex, auditory cortex, striatum, and visual cortex (high self-recovery rate) (Table 2 **and** Fig. 4). The results also indicated that the SERT self-recovery in rat brain after MDMA-induction was time-dependent and returned to 70.7% ± 3.96% of baseline values at day 28. The regions of low or mid-self-recovery rate were the most affected region by MDMA [4, 45].

In contrast, MacGregor et al., (2003) reported a clear loss of SERT binding sites in rats 3 months after administering the high-dose MDMA regime (4 × 5 mg/kg over 4 h in 2 consecutive days) [12], This agrees with numerous previous studies that show a SERT loss in the cingulate cortex, hippocampus, entorhinal

cortex, medial hypothalamic area, and the medial and lateral thalamic nuclei of rats, following MDMA administration in a rodent model [46, 47]. Lew et al., (1996) reported that a progressive recovery of SERT binding was noted from 2 to 52 weeks following MDMA exposure [48]. Moreover, Li et al. (2010) reported < 50% SERT recovery rate using *in vivo* 4-[^{18}F]-ADAMPET in the midbrain, thalamus, hypothalamus, caudate-putamen, hippocampus, and frontal cortex at day 31 after MDMA administration [20].

The difference in recovery time-course between the present study and previous reports described above could be (1) methodological issues that affected the accuracy of the quantitative measurement. For example, the reports published before 2000 used quantitative autoradiographic to analyze tissue slices or high-performance liquid chromatography (HPLC) for homogeneous tissue. However, the present study used PET imaging. (2) The analysis techniques, i.e. the accuracy of PET and MRI-based atlases registration or the correction of partial volume effect could underestimate the SERT binding in small volumes.

In a primate study, Scheffel et al. (1998) showed that SERT binding increased from 40 days to 9 months after MDMA administration in the pons, midbrain, and hypothalamus. However, it decreased in cortical regions [49]. Ma et al., (2016) reported that the SERT recovery rate was on average of ~ 66.6% and ~ 68.6% after MDMA administration in the striatum, thalamus, and midbrain at 24 and 54 months, respectively [13].

In human studies, some studies examined the reversibility of the SERT binding during abstinence from MDMA administration. Several reports demonstrated no difference in SERT binding between former ecstasy users and drug-naive controls after 1 year of abstinence [50, 51, 52].

Some preclinical or clinical studies confirmed a recovery in SERT binding after MDMA administration [40]. However, the question raised is the correlation between recovery of SERT binding and the function of SERT neurons. In the rat model, Andó et al. reported that 6 months after administering high-dose (15 or 30mg/kg, i.p), MDMA-induced damage of serotonergic axons showed recovery in most brain areas. However, SSRIs reduce serotonergic functions. Anxiety and aggression remain altered [53]. Li et al., (2010) suggested that when the SERT recovery rate reached ~ 35.2% compared to the controls, the density of serotonergic fibers and cell bodies decreased at day 31 after MDMA treatment (10 mg/kg, i.p) [20].

In the human study, several studies reported that after one year of abstinence, ex-MDMA users showed deficits in the Rey Auditory Verbal Learning Test similar to current MDMA users although SERT binding was similar to control level [50]. A review of empirical research (2013) supported those cognitive impairments following MDMA administration, which could result in a long-term cognitive effect, such as retrospective memory, prospective memory, higher cognition, problem-solving, and social intelligence. It can also result to sleep architecture, sleep apnoea, complex vision, pain, neurohormones, and psychiatric status [54].

Golding et al., (2007) reported that light ecstasy users showed a small significant cognitive impairment. However, no such impairment was detected among ex-users absent from the drug for at least 6 months [55]. Thus, neuroimaging studies show reduced serotonin transporter levels across the cerebral cortex, associated with neurocognitive impairments. SERT recovery positively correlates with the duration of MDMA abstinence. However, it is unclear whether the cause is associated with the SERT neurons recovery or other causes. Future longitudinal studies are recommended to investigate the serotonin level in blood or cerebrospinal fluid [45] or behavior tests.

The present results demonstrated that co-administration of MDMA with AMI rapidly blocked MDMA-induced serotonin release and MDMA neurotoxicity, restored globally, and largely accelerated SERT levels at day 14. After day 14, the progression of SERT recovery rate increased slowly at a rate of approximately 3% per 7 days and reached ~ 70% of baseline at day 28. Among all regions, those regions with low or mid-self-recovery rates had weaker responses to AMI when compared to regions with high recovery rates.

Li et al., (2010) reported that co-administration of MDMA with SSRI, fluoxetine, restored SERT binding rate to ~ 79.6 % of the control level at day 31 post-MDMA [20]. Compared to fluoxetine in the current results, AMI showed a 84.38% ± 2.05% of recovery rate at day 28. AMI had a higher neuroprotective effect because of its antiapoptotic effect that prevented PC12 cell death caused by hydrogen peroxide [56]. Another reason could be that MDMA can cause hyponatremia that induces seizures [57], resulting in an anoxic brain. However, AMI can protect primary cultured hippocampal neurons and *in vivo* hippocampal neurons from oxygen-glucose deprivation-induced apoptosis [34]. Moreover, AMI showed significant improvement in long- and short-term memory and increased neurogenesis and neurosynaptic marker proteins in an AD mouse model [32]. However, MDMA can influence a long impact on cognitive impairments.

Cytochrome P450 2D6 is the main enzyme involved in MDMA metabolism [58], and the AMI is a potent inhibitor of the Cytochrome P450 2D6 enzyme [59], which may inhibit MDMA metabolism and increase the MDMA toxicity.

In contrast to the expensive, risk-overt, and time-consuming nature of de novo drug development, a more effective approach is to apply the well-tolerated, therapeutics in new pharmacogenomic settings. Seeking effective treatments in Food and Drug Administration-approved drugs has become a promising drug discovery route for neuroprotection by MDMA.

Our findings in immunochemical staining confirmed the PET study, revealing that at day 28 post-MDMA, the density of serotonergic fibers and cell bodies decreased in the MDMA group. On the contrary, co-administration of MDMA with AMI showed improvement in structural damage of serotonin neurons (Fig. 5–6). After being measured by RT-PCR, our results supported a decrease in SERT gene expression in the striatum, parietal cortex, and hippocampus after MDMA treatment [60]. The results were consistent with several studies that reported dramatic decreases in SERT binding following various MDMA dosing regimens and post-administration [61]. This previous study also showed the effect of MDMA on SERT depletion region-specific. For example, areas such as the striatum, raphe nuclei seem to affect stronger

than other areas such as the hypothalamus. In the long term, the evidence suggests that SERT gene expression is negatively regulated by MDMA exposure [62], leading to reductions in SERT binding and immunoreactive fiber density in the absence of physical damage.

Conclusions

Based on the longitudinal *in vivo* 4-[^{18}F]-ADAM PET, the present study found a clear loss of SERT binding sites in rats after the low-dose MDMA regime. We demonstrated that SERT recovery was positively correlated to the MDMA abstinence duration, implying that the lower SERT densities in MDMA-induced rats reflected neurotoxic effects, which varied by region-specific and reversible. Current data also supported that AMI might have neuroprotective effects that globally accelerated the recovery rate of SERT besides its anti-depressive effects. Future studies should verify the neuroprotective effects of AMI in neuronal cells.

Abbreviations

MDMA: 4-Methylenedioxymethamphetamine

SERT: serotonin reuptake transporter

AMI: amitriptyline

4-[^{18}F]-ADAM: N,N-Dimethyl-2-(2Amino4-18F-Fluorophenylthio)- Benzylamine

SSRIs: selective serotonin reuptake inhibitors

NET: norepinephrine transport

DAT: dopamine transport

HPLC: high-performance liquid chromatography

SUV: standardized uptake value

IHC: Immunohistochemistry

Declarations

Ethics approval: All animal handling procedures were approved by National Defense Medical Center (IAUIC No 10-093) and animal study was performed according to the Guidelines for Animal Experimentation of National Defense Medical Center.

Consent for publication

Not applicable.

Availability of data and material

The authors confirm that the data supporting the findings of this study are available within the article.

Conflicts of Interests

The authors have no financial or competing interests to declare.

Funding

Funding for this study was provided by Ministry of Science and Technology R.O.C. (MOST-109-2314-B-038-151, MOST-110-2314-B-A49A-528) and The Featured Areas Research Center Program within the framework of the Higher Education Sprout Project by the Ministry of Education (MOE) in Taiwan.

Authors contributions: Conceptualization, K.H. M., and W.S. H., Investigation, C.H. C., Y.Y. K., C.J. T., and T.H. Y., Data analysis, T.H. Y., Writing and editing, S.H.H. Y., Funding Acquisition, K.H. M., and W.S. H. All authors read and approved the final manuscript.

Acknowledgements

We thank the Molecular Imaging Facility Small Animal 7T PET/MR and Brain Research Center at National Yang Ming Chaio Tung University for the technical support.

References

1. Lyles J, Cadet JL. Methylenedioxymethamphetamine (MDMA, Ecstasy) neurotoxicity: cellular and molecular mechanisms. Brain Res Brain Res Rev. 2003;42(2):155–68.
2. Capela JP, Carmo H, Remiao F, Bastos ML, Meisel A, Carvalho F. Molecular and cellular mechanisms of ecstasy-induced neurotoxicity: an overview. Mol Neurobiol. 2009;39(3):210–71.
3. Schmidt CJ. Neurotoxicity of the psychedelic amphetamine, methylenedioxymethamphetamine. J Pharmacol Exp Ther. 1987;240(1):1–7.
4. Baumann MH, Wang X, Rothman RB. 3,4-Methylenedioxymethamphetamine (MDMA) neurotoxicity in rats: a reappraisal of past and present findings. Psychopharmacology. 2007;189(4):407–24.
5. Verrico CD, Miller GM, Madras BK. MDMA (Ecstasy) and human dopamine, norepinephrine, and serotonin transporters: implications for MDMA-induced neurotoxicity and treatment. Psychopharmacology. 2007;189(4):489–503.
6. Nakagawa T, Otsubo Y, Yatani Y, Shirakawa H, Kaneko S. Mechanisms of substrate transport-induced clustering of a glial glutamate transporter GLT-1 in astroglial-neuronal cultures. Eur J Neurosci. 2008;28(9):1719–30.

7. Chu T, Kumagai Y, DiStefano EW, Cho AK. Disposition of methylenedioxymethamphetamine and three metabolites in the brains of different rat strains and their possible roles in acute serotonin depletion. Biochem Pharmacol. 1996;51(6):789–96.
8. Bhide NS, Lipton JW, Cunningham JI, Yamamoto BK, Gudelsky GA. Repeated exposure to MDMA provides neuroprotection against subsequent MDMA-induced serotonin depletion in brain. Brain Res. 2009;1286:32–41.
9. Huff C, Bhide N, Schroering A, Yamamoto BK, Gudelsky GA. Effect of repeated exposure to MDMA on the function of the 5-HT transporter as assessed by synaptosomal 5-HT uptake. Brain Res Bull. 2013;91:52–7.
10. Aguirre N, Barrionuevo M, Lasheras B, Del Rio J. The role of dopaminergic systems in the perinatal sensitivity to 3, 4-methylenedioxymethamphetamine-induced neurotoxicity in rats. J Pharmacol Exp Ther. 1998;286(3):1159–65.
11. Ricaurte GA. Studies of MDMA-induced neurotoxicity in nonhuman primates: a basis for evaluating long-term effects in humans. NIDA Res Monogr. 1989;94:306–22.
12. McGregor IS, Clemens KJ, Van der Plasse G, Li KM, Hunt GE, Chen F, et al. Increased anxiety 3 months after brief exposure to MDMA ("Ecstasy") in rats: association with altered 5-HT transporter and receptor density. Neuropsychopharmacology. 2003;28(8):1472–84.
13. Ma KH, Liu TT, Weng SJ, Chen CF, Huang YS, Chueh SH, et al. Effects of dextromethorphan on MDMA-induced serotonergic aberration in the brains of non-human primates using [(123)I]-ADAM/SPECT. Sci Rep. 2016;6:38695.
14. Vollenweider FX, Gamma A, Liechti M, Huber T. Psychological and cardiovascular effects and short-term sequelae of MDMA ("ecstasy") in MDMA-naive healthy volunteers. Neuropsychopharmacology. 1998;19(4):241–51.
15. Kirilly E. Long-term neuronal damage and recovery after a single dose of MDMA: expression and distribution of serotonin transporter in the rat brain. Neuropsychopharmacol Hung. 2010;12(3):413–23.
16. McCann UD, Szabo Z, Seckin E, Rosenblatt P, Mathews WB, Ravert HT, et al. Quantitative PET studies of the serotonin transporter in MDMA users and controls using [11C]McN5652 and [11C]DASB. Neuropsychopharmacology. 2005;30(9):1741–50.
17. McCann UD, Szabo Z, Vranesic M, Palermo M, Mathews WB, Ravert HT, et al. Positron emission tomographic studies of brain dopamine and serotonin transporters in abstinent (+/-)3,4-methylenedioxymethamphetamine ("ecstasy") users: relationship to cognitive performance. Psychopharmacology. 2008;200(3):439–50.
18. Sanchez V, Camarero J, Esteban B, Peter MJ, Green AR, Colado MI. The mechanisms involved in the long-lasting neuroprotective effect of fluoxetine against MDMA ('ecstasy')-induced degeneration of 5-HT nerve endings in rat brain. Br J Pharmacol. 2001;134(1):46–57.
19. Renoir T, Paizanis E, El Yacoubi M, Saurini F, Hanoun N, Melfort M, et al. Differential long-term effects of MDMA on the serotoninergic system and hippocampal cell proliferation in 5-HTT knock-out vs.

wild-type mice. Int J Neuropsychopharmacol. 2008;11(8):1149–62.

20. Li IH, Huang WS, Shiue CY, Huang YY, Liu RS, Chyueh SC, et al. Study on the neuroprotective effect of fluoxetine against MDMA-induced neurotoxicity on the serotonin transporter in rat brain using micro-PET. Neuroimage. 2010;49(2):1259–70.
21. Berger UV, Gu XF, Azmitia EC. The substituted amphetamines 3,4-methylenedioxymethamphetamine, methamphetamine, p-chloroamphetamine and fenfluramine induce 5-hydroxytryptamine release via a common mechanism blocked by fluoxetine and cocaine. Eur J Pharmacol. 1992;215(2–3):153–60.
22. Shankaran M, Gudelsky GA. A neurotoxic regimen of MDMA suppresses behavioral, thermal and neurochemical responses to subsequent MDMA administration. Psychopharmacology. 1999;147(1):66–72.
23. Battaglia G, Yeh SY, De Souza EB. MDMA-induced neurotoxicity: parameters of degeneration and recovery of brain serotonin neurons. Pharmacol Biochem Behav. 1988;29(2):269–74.
24. Gorska AM, Kaminska K, Wawrzczak-Bargiela A, Costa G, Morelli M, Przewlocki R, et al. Neurochemical and Neurotoxic Effects of MDMA (Ecstasy) and Caffeine After Chronic Combined Administration in Mice. Neurotox Res. 2018;33(3):532–48.
25. Budzynska B, Wnorowski A, Kaszubska K, Biala G, Kruk-Slomka M, Kurzepa J, et al. Acute MDMA and Nicotine Co-administration: Behavioral Effects and Oxidative Stress Processes in Mice. Front Behav Neurosci. 2018;12:149.
26. Tatsumi M, Groshan K, Blakely RD, Richelson E. Pharmacological profile of antidepressants and related compounds at human monoamine transporters. Eur J Pharmacol. 1997;340(2–3):249–58.
27. Sharma H, Santra S, Dutta A. Triple reuptake inhibitors as potential next-generation antidepressants: a new hope? Future Med Chem. 2015;7(17):2385–406.
28. Leucht C, Huhn M, Leucht S. Amitriptyline versus placebo for major depressive disorder. Cochrane Database Syst Rev. 2012;12:CD009138.
29. Moore RA, Derry S, Aldington D, Cole P, Wiffen PJ. Amitriptyline for neuropathic pain in adults. Cochrane Database Syst Rev. 2015(7):CD008242.
30. Anderson IM. Selective serotonin reuptake inhibitors versus tricyclic antidepressants: a meta-analysis of efficacy and tolerability. J Affect Disord. 2000;58(1):19–36.
31. Barbui C, Hotopf M. Amitriptyline v. the rest: still the leading antidepressant after 40 years of randomised controlled trials. Br J Psychiatry. 2001;178:129–44.
32. Chadwick W, Mitchell N, Caroll J, Zhou Y, Park SS, Wang L, et al. Amitriptyline-mediated cognitive enhancement in aged 3xTg Alzheimer's disease mice is associated with neurogenesis and neurotrophic activity. PLoS One. 2011;6(6):e21660.
33. Xu H, Steven Richardson J, Li XM. Dose-related effects of chronic antidepressants on neuroprotective proteins BDNF, Bcl-2 and Cu/Zn-SOD in rat hippocampus. Neuropsychopharmacology. 2003;28(1):53–62.

34. Jang SW, Liu X, Chan CB, Weinshenker D, Hall RA, Xiao G, et al. Amitriptyline is a TrkA and TrkB receptor agonist that promotes TrkA/TrkB heterodimerization and has potent neurotrophic activity. Chem Biol. 2009;16(6):644–56.
35. Kaminska K, Lenda T, Konieczny J, Wardas J, Lorenc-Koci E. Interactions of the tricyclic antidepressant drug amitriptyline with L-DOPA in the striatum and substantia nigra of unilaterally 6-OHDA-lesioned rats. Relevance to motor dysfunction in Parkinson's disease. Neurochem Int. 2018;121:125–39.
36. Ma KH, Huang WS, Kuo YY, Peng CJ, Liou NH, Liu RS, et al. Validation of 4-[18F]-ADAM as a SERT imaging agent using micro-PET and autoradiography. Neuroimage. 2009;45(3):687–93.
37. Huang YY, Huang WS, Chu TC, Shiue CY. An improved synthesis of 4-[18F]-ADAM, a potent serotonin transporter imaging agent. Appl Radiat Isot. 2009;67(6):1063–7.
38. Huang YY, Huang WS, Ma KH, Chou TK, Kuo YY, Cheng CY, et al. Synthesis and comparison of 4-[18F]F-ADAM, 2-[18F]F-ADAM, N-Desmethyl-4-[18F]F-ADAM and [18F]F-AFM as serotonin transporter imaging agents. Appl Radiat Isot. 2012;70(10):2298–307.
39. Chen YA, Huang WS, Lin YS, Cheng CY, Liu RS, Wang SJ, et al. Characterization of 4-[18F]-ADAM as an imaging agent for SERT in non-human primate brain using PET: a dynamic study. Nucl Med Biol. 2012;39(2):279–85.
40. Shih JH, Ma KH, Chen CF, Cheng CY, Pao LH, Weng SJ, et al. Evaluation of brain SERT occupancy by resveratrol against MDMA-induced neurobiological and behavioral changes in rats: A 4-[(1)(8)F]-ADAM/small-animal PET study. Eur Neuropsychopharmacol. 2016;26(1):92–104.
41. Huang WS, Huang SY, Ho PS, Ma KH, Huang YY, Yeh CB, et al. PET imaging of the brain serotonin transporters (SERT) with N,N-dimethyl-2-(2-amino-4-[18F]fluorophenylthio)benzylamine (4-[18F]-ADAM) in humans: a preliminary study. Eur J Nucl Med Mol Imaging. 2013;40(1):115–24.
42. de Win MM, de Jeu RA, de Bruin K, Habraken JB, Reneman L, Booij J, et al. Validity of in vivo [123I]beta-CIT SPECT in detecting MDMA-induced neurotoxicity in rats. Eur Neuropsychopharmacol. 2004;14(3):185–9.
43. Klomp A, den Hollander B, de Bruin K, Booij J, Reneman L. The effects of ecstasy (MDMA) on brain serotonin transporters are dependent on age-of-first exposure in recreational users and animals. PLoS One. 2012;7(10):e47524.
44. Laabbar W, Elgot A, Kissani N, Gamrani H. Chronic aluminum intoxication in rat induced both serotonin changes in the dorsal raphe nucleus and alteration of glycoprotein secretion in the subcommissural organ: Immunohistochemical study. Neurosci Lett. 2014;577:72–6.
45. Mustafa NS, Bakar NHA, Mohamad N, Adnan LHM, Fauzi N, Thoarlim A, et al. MDMA and the Brain: A Short Review on the Role of Neurotransmitters in Neurotoxicity. Basic Clin Neurosci. 2020;11(4):381–8.
46. Boot BP, Mechan AO, McCann UD, Ricaurte GA. MDMA- and p-chlorophenylalanine-induced reduction in 5-HT concentrations: effects on serotonin transporter densities. Eur J Pharmacol. 2002;453(2–3):239–44.

47. Harkin A, Connor TJ, Mulrooney J, Kelly JP, Leonard BE. Prior exposure to methylenedioxyamphetamine (MDA) induces serotonergic loss and changes in spontaneous exploratory and amphetamine-induced behaviors in rats. Life Sci. 2001;68(12):1367–82.
48. Lew R, Sabol KE, Chou C, Vosmer GL, Richards J, Seiden LS. Methylenedioxymethamphetamine-induced serotonin deficits are followed by partial recovery over a 52-week period. Part II: Radioligand binding and autoradiography studies. J Pharmacol Exp Ther. 1996;276(2):855–65.
49. Scheffel U, Szabo Z, Mathews WB, Finley PA, Dannals RF, Ravert HT, et al. In vivo detection of short- and long-term MDMA neurotoxicity–a positron emission tomography study in the living baboon brain. Synapse. 1998;29(2):183–92.
50. Reneman L, Lavalaye J, Schmand B, de Wolff FA, van den Brink W, den Heeten GJ, et al. Cortical serotonin transporter density and verbal memory in individuals who stopped using 3,4-methylenedioxymethamphetamine (MDMA or "ecstasy"): preliminary findings. Arch Gen Psychiatry. 2001;58(10):901–6.
51. Buchert R, Thomasius R, Wilke F, Petersen K, Nebeling B, Obrocki J, et al. A voxel-based PET investigation of the long-term effects of "Ecstasy" consumption on brain serotonin transporters. Am J Psychiatry. 2004;161(7):1181–9.
52. Selvaraj S, Hoshi R, Bhagwagar Z, Murthy NV, Hinz R, Cowen P, et al. Brain serotonin transporter binding in former users of MDMA ('ecstasy'). Br J Psychiatry. 2009;194(4):355–9.
53. Ando RD, Adori C, Kirilly E, Molnar E, Kovacs GG, Ferrington L, et al. Acute SSRI-induced anxiogenic and brain metabolic effects are attenuated 6 months after initial MDMA-induced depletion. Behav Brain Res. 2010;207(2):280–9.
54. Parrott AC. Human psychobiology of MDMA or 'Ecstasy': an overview of 25 years of empirical research. Hum Psychopharmacol. 2013;28(4):289–307.
55. Golding JF, Groome DH, Rycroft N, Denton Z. Cognitive performance in light current users and ex-users of ecstasy (MDMA) and controls. Am J Drug Alcohol Abuse. 2007;33(2):301–7.
56. Kolla N, Wei Z, Richardson JS, Li XM. Amitriptyline and fluoxetine protect PC12 cells from cell death induced by hydrogen peroxide. J Psychiatry Neurosci. 2005;30(3):196–201.
57. Giorgi FS, Lazzeri G, Natale G, Iudice A, Ruggieri S, Paparelli A, et al. MDMA and seizures: a dangerous liaison? Ann N Y Acad Sci. 2006;1074:357–64.
58. de la Torre R, Yubero-Lahoz S, Pardo-Lozano R, Farre M. MDMA, methamphetamine, and CYP2D6 pharmacogenetics: what is clinically relevant? Front Genet. 2012;3:235.
59. Dean L. Amitriptyline Therapy and CYP2D6 and CYP2C19 Genotype. In: Pratt VM, Scott SA, Pirmohamed M, Esquivel B, Kane MS, Kattman BL, et al., editors. Medical Genetics Summaries. Bethesda (MD)2012.
60. Biezonski DK, Meyer JS. Effects of 3,4-methylenedioxymethamphetamine (MDMA) on serotonin transporter and vesicular monoamine transporter 2 protein and gene expression in rats: implications for MDMA neurotoxicity. J Neurochem. 2010;112(4):951–62.

61. Green AR, Mechan AO, Elliott JM, O'Shea E, Colado MI. The pharmacology and clinical pharmacology of 3,4-methylenedioxymethamphetamine (MDMA, "ecstasy"). Pharmacol Rev. 2003;55(3):463–508.
62. Kirilly E, Molnar E, Balogh B, Kantor S, Hansson SR, Palkovits M, et al. Decrease in REM latency and changes in sleep quality parallel serotonergic damage and recovery after MDMA: a longitudinal study over 180 days. Int J Neuropsychopharmacol. 2008;11(6):795–809.

Tables

Due to technical limitations, table 1 and 2 is only available as a download in the Supplemental Files section.

Figures

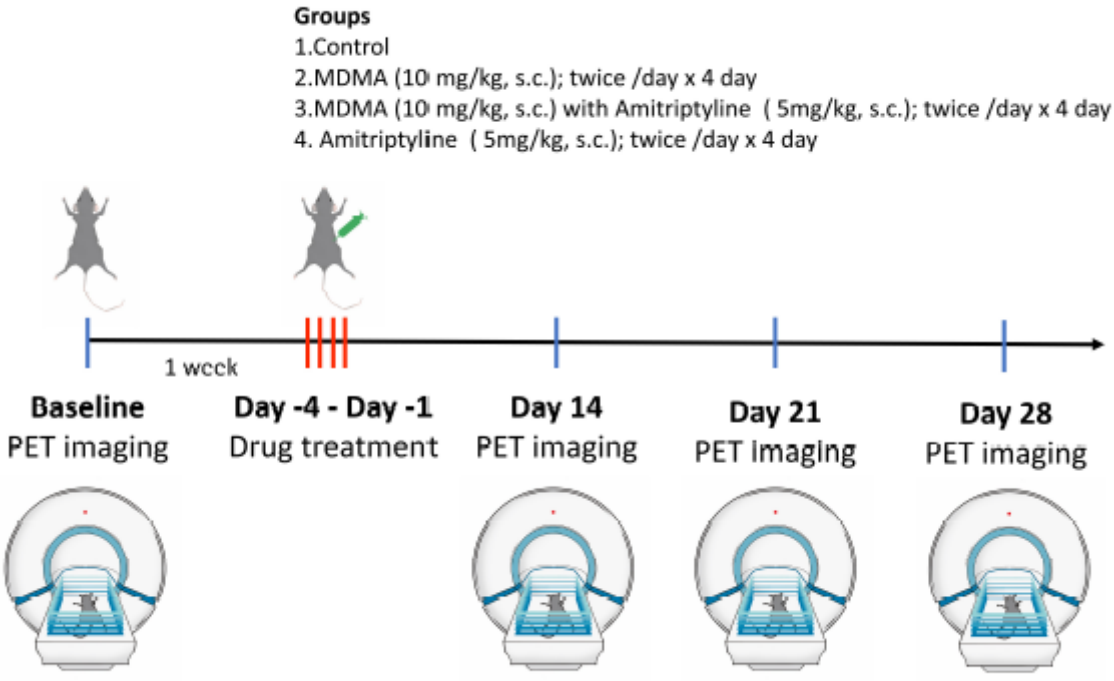

Figure 1

Schematic and graphical representation of the study design. A total of 24 rats received 4-[18F]-ADAM PET imaging as a baseline. One week later, animals were randomly grouped into 4: Group 1 as a control, Group 2 MDMA, Group 3 AMI with MDMA, Group 4 AMI alone. Rats received drug treatment twice daily on days 1, 2, 3, 4. Then, 4-[18F]-ADAM micro-PET imaging was performed on days 14, 21, 28, and immunohistochemistry was performed on day 30.

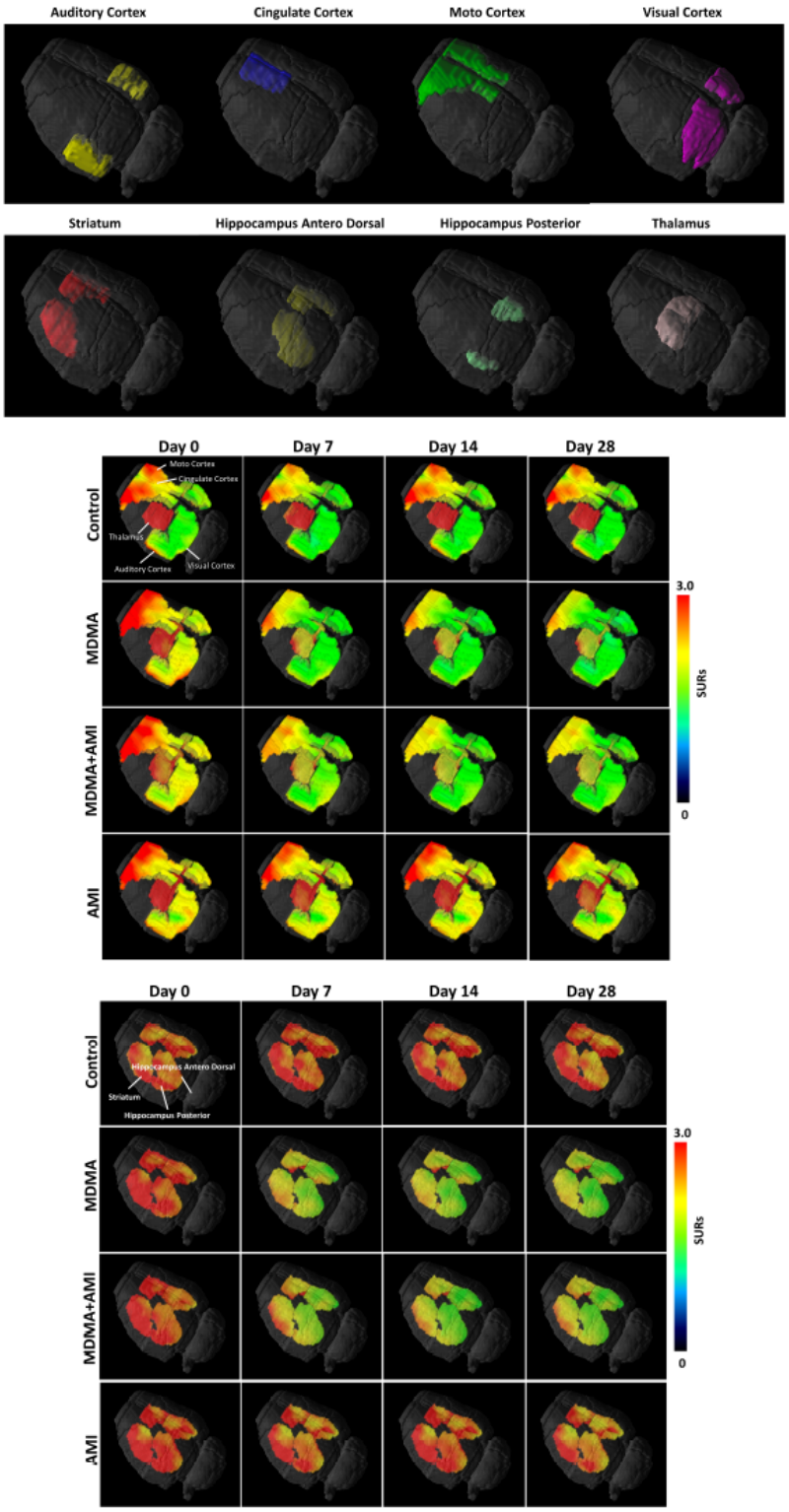

Figure 2

3D 4-[18F]-ADAM PET images (A) Illustration of the location of the brain regions was used to estimate the SERT binding of 4-[18F]-ADAM, (B) 4-[18F]-ADAM binding to SERT shown in the motor cortex, cingulate cortex, auditory cortex, visual cortex, and thalamus, (C) 4-[18F]-ADAM binding to SERT shown in the striatum, hippocampus, and hippocampus anterodorsal.

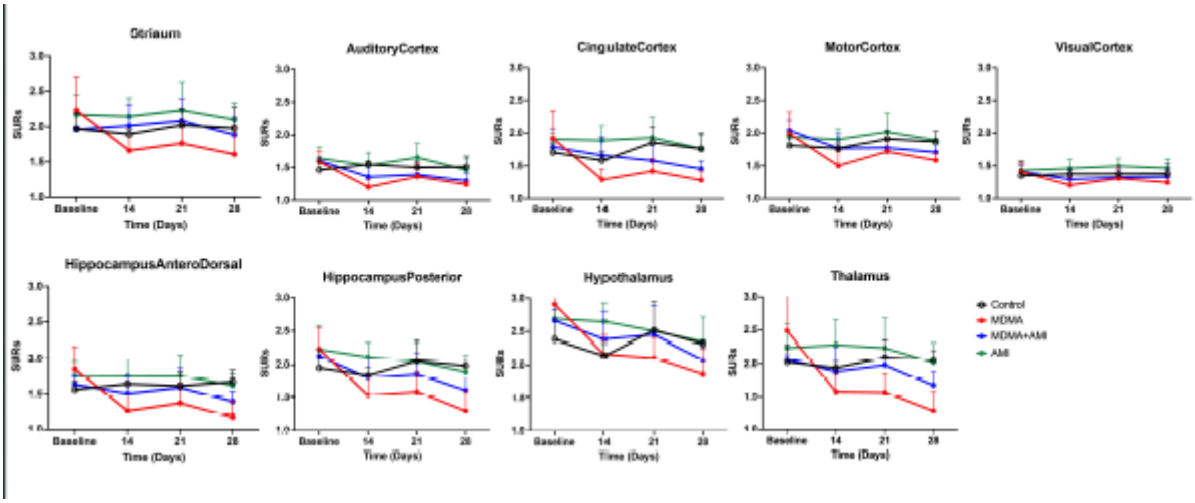

Figure 3

Specific uptake ratios (SURs) of 4-[18F]-ADAM of baseline and on day 7, 14 and 28 from the beginning of the 4-day treatment in rat brain regions. 4-[18F]-ADAM distribution in the different brain regions after intraperitoneal administration of different drug groups. Compared to the control (black line), MDMA produced a significant reduction of 4-[18F]-ADAM binding to SERT from day 14, progressively increased up to day 28 (red line). The group of AMI with MDMA (blue line) showed the neuroprotective effect from day 14, with no statistical difference with the control. The control and AMI alone (green line) groups showed a similar pattern. Data are mean ± SD.

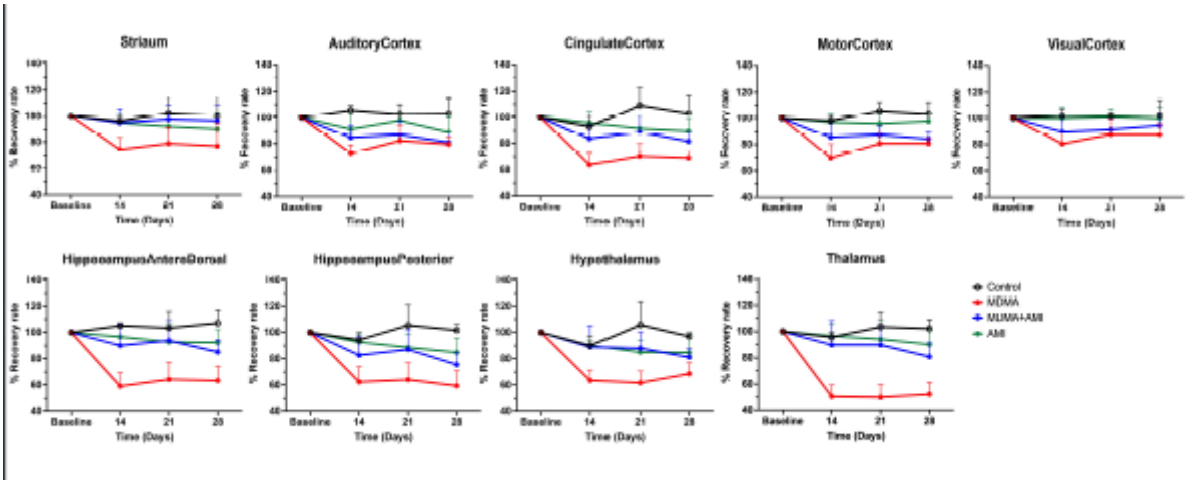

Figure 4

Comparison of recovery rate, based on graphical analyses of 4-[18F]-ADAM binding before and after drug administration. Among four groups, the MDMA group (red line) appeared the lowest recovery rate at day 14, slightly increased at day 21, and recovered to ~70% of baseline value at day 28. AMI with MDMA (blue line) significantly accelerated the recovery rate from day 14 and slowly increased up to day 28 when compared with the MDMA group. The control and AMI alone (green line) groups showed no difference in curve tendency. Data are mean ± SD.

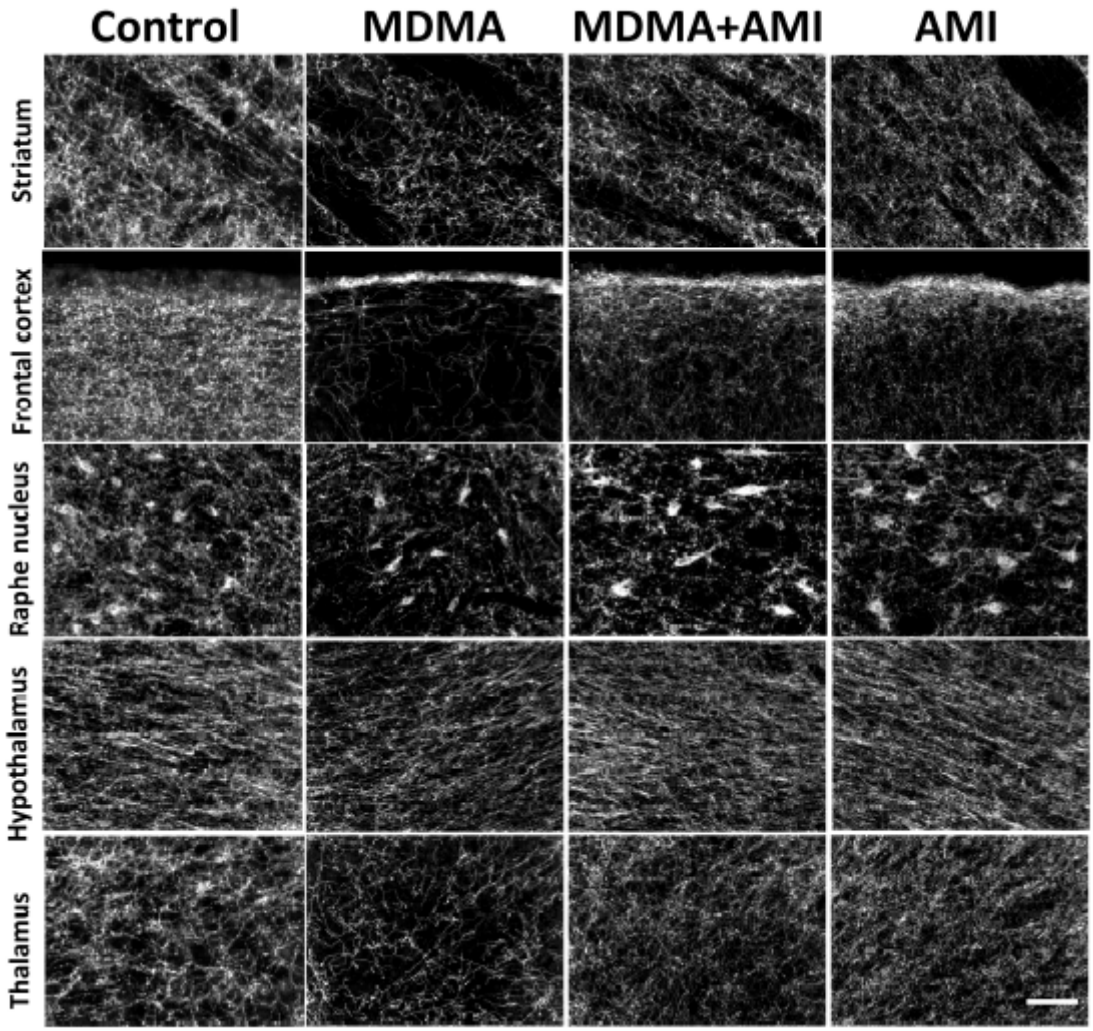

Figure 5

Dark-field photomicrograph of SERT immunoreactivity in different brain regions after drug treatment. Compared to the control, SERT immunoreactivity was significantly lower in the MDMA group, slightly lower in AMI with the MDMA group, and almost equal in the AMI alone group. Scale bar, 100 μm.

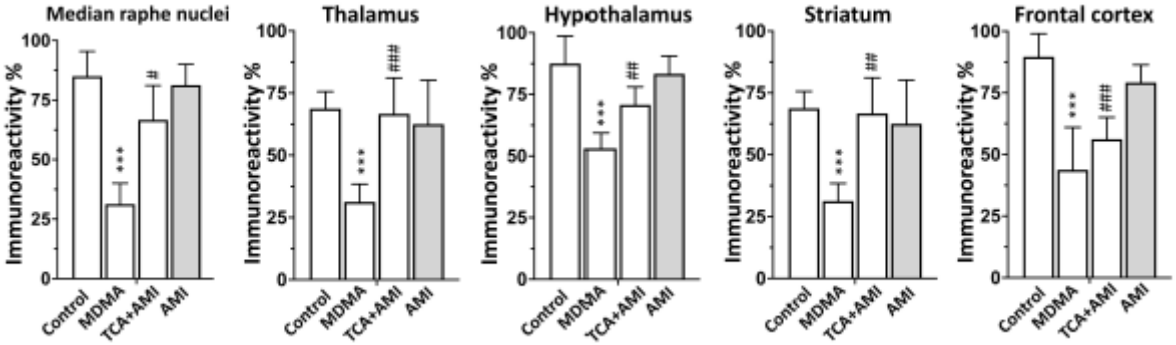

Figure 6

Quantification of SERT immunoreactivity in the brain regions (based on the data in Fig. 5). Data are mean ± SD. Values, different superscript letters indicate significant differences (***P < 0.005 compared to controls; ##P < 0.01, ###P < 0.005, Group C- amitriptyline with MDMA vs. Group B- MDMA).

Supplementary Files

This is a list of supplementary files associated with this preprint. Click to download.

- Onlinefloatimage2.png
- Onlinefloatimage3.png